Analysis on Regular Rotational Gait of a Quadruped Walking Robot

Whee Kuk Kim, Whang Cho, Byung-Ju Yi

Abstract: In this paper, the regular rotational gaits of the quadruped crawling robot are studied. It is assumed that the proposed regular rotational gaits starts from one of six support patterns in a translational gaits and end up with one of six support patterns in a translational gaits. Noting that six support patterns in a regular translational gait belong to two different groups with respect to regular rotational gait, the static stability margin and the maximum rotational displacement during one rotational stride period for the two representative support patterns are investigated. It is expected that the proposed regular rotational gaits will enhance the omni-directional characteristics of the quadruped crawling robot.

Keywords: omni-directional characteristic, crawling robot, stability margin, foothold region

I. Introduction

Most of design and gaits of the walking robot developed up to now emulates the biological study results on insects or animals.[1,2,3] Crawling, pacing, trotting, galloping, running, hopping, bouncing, etc. are types of walking observed from the insects and animals.[2]

Walking of robots is classified as two categories such as static walking and dynamic walking, depending on whether or not static balance of the robot is maintained during working. Particularly, static walking is observed from crawling of insects or animals with more than four legs when they move at a slow speed. It can be observed that in crawling, the static balance is always maintained by placing the supporting legs such that the mass center of the moving objects is inside the convex which is formed by connecting the foothold points.[4] When fast walking is required, inertial effects are considered by defining an active mass center.[5]

There are two different types of gaits; translational gaits and rotational gaits.[1] In translational gaits, the robot moves forwards or backwards. In rotational gaits, the robot rotates its body about its mass center. When the quadruped walking robot moves via. static walking, either the regular gaits or the free gaits are used depending on the condition of the road.

In this study, the regular rotational gaits of the quadruped walking robot are investigated. With this rotational gaits, only the robot changes its support patterns without changing its orientation of the body, by moving legs to change their foothold positions. Therefore, the proposed regular rotational gaits always end up with one of six support patterns in a regular translational gaits.[1] Thereby, after performing this regular rotational gaits, the quadruped walking robot can immediately continue to perform the regular (translational) gait along the given direction.

This paper can be summarized as follows. Firstly, the structure of the quadruped walking robot under investigation and one type of the regular (translational) gaits of the quadruped walking robot which have six different support patterns are described. Then, the regular rotational gaits corresponding to two representative patterns out of six patterns are proposed. Lastly, the maximum static stability margin, which is defined as the shortest length along the moving direction from the mass center of the robot to the line segments of the convex, and the maximum amount of rotational displacement of the regular rotational gaits are investigated.

Manuscript received: May 20, 2001, Accepted: Aug. 27, 2001.

Whee Kuk Kim: Department of Control and Instrumenttation Engineering, Korea University 208 Seochang-dong, Chochiwon-up, Yongi-kun, Chungnam-do, 339-700, Korea.(wheekuk@korea.ac.kr)

Whang Cho: Department of Information and Control Kwangwoon University, Wolgye-dong Nowon-ku, 447-1, 132-701, Seoul, Korea.(robot@daisy.kwangwoon.ac.kr)

Byung-Ju Yi: School of Electrical Engineering and Computer Science Hanyang University, 1271, San 1-Dong, Ansan, Kyunggi-do, 425-791, Korea.(bj@hanyang.ac.kr)

II. A quadruped walking robot

Fig. 1 shows the quadruped walking robot under study. Mass center of the robot is at the geometric center of the body. Consider the local frame (x y z) fixed on the body of the robot and with its origin at the mass center of the robot as shown in Fig. 2. Each of four legs consists of a revolute joint which is located at a distance e from the center of the body and two prismatic joints which move in the local $x-y$ plane parallel to the body plane. For simplicity, it is assumed that the robot maintains the orientation of its body parallel to the ground during walking. Therefore, each foothold region of four legs of the quadruped walking robot can be represented as a projected region to the ground which is inside a circle of radius of R with its center at the intersection between the ground and the first joint axis as shown in Fig. 2.

Assume that the walking robot moves along the y axis. When the walking robot moves forward in a regular gait, the foothold position is located along the line segment which is

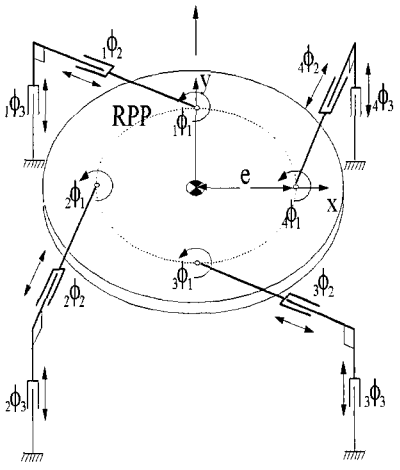

Fig. 1. Quadruped walking robot.

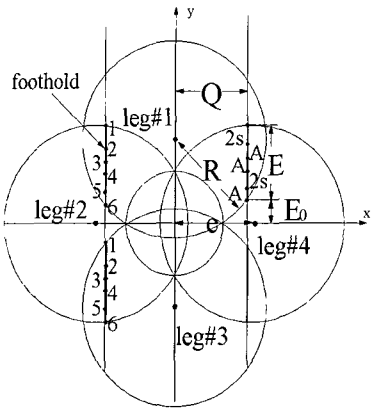

Fig. 2. Top view of a quadruped walking robot with eccentrically located legs.

parallel to the y axis and apart from the distance Q from the x xis. Along this line segment within a foothold region, the corresponding leg can be placed. Denote the length of the line segment as E and the unreachable foothold length on which leg can not be placed as E_o , respectively, as in Fig. 2. And denote the static stability margin of the robot as s. It can be noted that when the robot moves in an arbitrary direction in a regular translational gait, the robot has different magnitudes of stride length along each direction.

Consider that the regular gait presented by Lee and Shih[1]. The consequent steps in one stride period of the robot with stability margin s can be summarized as in Table 1. From table 1, the stride length λ can be represented as

$$\lambda = 4A(s) + 4s \tag{1}$$

and the foothold length of each leg E can be obtained as follows.

$$E = 3A(s) + 4(s) \tag{2}$$

In (1) and (2), $A(s)$ represents the amount of forward movement of the walking robot securing the stability margin of s while one leg is off the ground.

In a regular gait, there exist six different support patterns in one stride period. Between these patterns the robot moves the distance of either $A(s)$ or $2s$. More specifically, starting from the support pattern #1, with each of four legs of the walking robot fixed on the ground at the specified foothold position, 1, 4, 2, and 5, as shown n Figure 2, respectively, the body of the walking robot moves forward the distance of $2s$.

At the end of this motion, the robot reaches to the support pattern #2 where each of four legs is at foothold position of 2, 5, 3, and 6, respectively. Note that since the foothold position is represented with respect to the body of the walking robot, the forward movement of the robot is reflected as the backward movement of the foothold position in the Figure. Starting from this support pattern #2, while leg #3 at foothold position 6 is lifted and placed at the foothold position 1, the body of the robot moves forward an distance of $A(s)$ to reach to the support pattern #3. The rest of procedures is similar. Fig. 3a)-3f) represents the six support patterns corresponding to the ones shown in table 1.

Table 1. Regular gait of a quadruped walking robot with static stability margin s

Support pattern #	1	2	3	4	5	6
Leg 1	1	2	3	4	5	6
Leg 2	4	5	6	1	2	3
Leg 3	5	6	1	2	3	4
Leg 4	2	3	4	5	6	1
Body motion	2s	A	A	2s	A	A
Transfer leg	x	3	2	x	4	1

x : there is no leg moving (fixed to the ground)

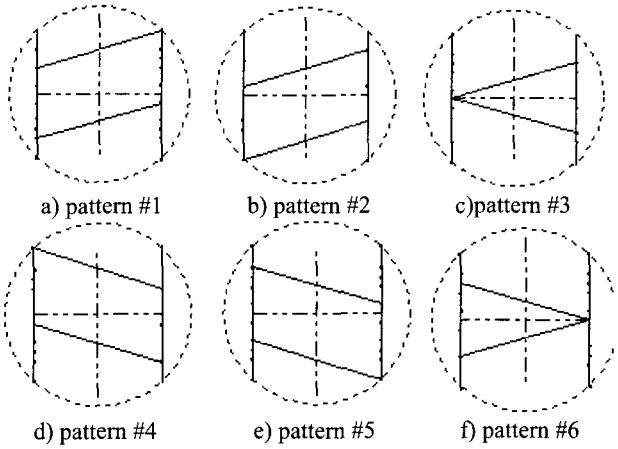

Fig. 3. Support patterns of a quadruped walking robot in regular gait.

III. Foothold length of the quadruped robot

Note that in Fig. 3, six support patterns can be categorized into two different groups noting that some of them are only the mirror images or symmetric images one another: that is, support patterns *1,2,4,* and *5* belong to one group and support patterns *3,* and *6* belong to the other group. Therefore, the results obtained from the investigation on one support pattern from each of two groups can be applied similarly to the other support pattern that belongs to the same group.

In this section, support pattern *1* and support pattern *6* are selected as representative support patterns for those two groups and their regular rotational gaits are proposed. And the maximum rotational angular displacement ($\Delta\theta max$) and maximum stability margin(s_{max}) for those two different support patterns are examined. For fixed $E + E_o$ but varying E_o , the maximum stability margin and the maximum rotational angular displacement are studied. And the maximum stability margin smax for given values of Q, E, E_o is obtained. Note that rotational gaits suggested in the paper are based on the assumption that it starts from one of six support pattern of regular gaits and at the end of the rotational gaits foothold position reaches one of six support patterns so that regular gaits could be performed immediately without going through any intermediate step. Thus, the robot can enter into the rotational gaits from any foothold support pattern during the cycle

of the translational gait. However, to change from the rotational gait to translational gait, its corresponding rotational gait cycle under operation should be completed.

Now, consider the support pattern ***6***. The regular rotational gaits is shown in Fig. 4a). Particularly, maximum stability margin ^{S}max can be obtained by considering the case that the robot rotates in an infinitesimal angular displacement as follows. In Fig. 4a), the equation of line $\overline{P_1P_5}$ can be represented as

$$y = \frac{2Eo + 5A + 6s}{2Q} x + \frac{A}{2} + s \tag{3}$$

It can be noted that the radius of an osculating circle with this line represents the maximum stability margin ^{S}max. Therefore, the maximum stability margin ^{S}max can be obtained as follow;

$$\begin{aligned} &4s^4 - 4(6Eo + 5E)s^3 + \{32Q^2 + \\ &(6Eo + 5E)^2\}s^2 - 4EQ^2s - E^2Q^2 = 0 \end{aligned} \tag{4}$$

Fig. 4a) and Fig. 4b) shows the order of movement of legs and the actual foothold positions during a regular rotational gait of the robot for a rotational of $\Delta\theta$, respectively. More specifically, the rotational gait starts from support pattern 6 (foothold positions of legs are 6 for leg #1, 3 for leg #2, 4 for leg #3, and 1 for leg #4) of the translational gaits and ends in the same support pattern 6 of translational gait as shown in Figure 4 where the new foothold position is marked by the arrow with the appropriate order number.

The robot begins to rotate from the support pattern ***6*** with $E_O \neq 0$ and maintains the given stability margin during the rotation. Once ^{S}max is found from eq. (4) for given E and E_o, using the condition that every foothold position should be located within the circle of radius of R with its center at the mass center of the robot, $\Delta\theta\, max$ can be expressed as below from Fig. 4b):

$$\Delta\theta_{max} = a\tan\left(\frac{y'_3}{x'_3}\right) + a\tan\left(\frac{Eo}{Q}\right) \tag{5}$$

where

$$x'_3 = \frac{-ab + \sqrt{a^2b^2 - (1+a^2)(b^2 - r^2)}}{1+a^2} \tag{6}$$

$$y'_3 = ax'_3 + b, \tag{7}$$

$$r = \sqrt{Q^2 + E^2{}_o}. \tag{8}$$

And when the line $\overline{P_4P'_3}$ represents the line osculating with the circle of radius of s with its origin at the mass center of the robot, a and b represent the slope and intersection point of the line $\overline{P_4P'_3}$, respectively, and they can be obtained as follows:

$$a = -\frac{x^*}{y^*}, \tag{9}$$

$$b = \frac{x^*}{y^*} x_4 + y_4, \tag{10}$$

$$y^* = \frac{s^2x_4 + s\sqrt{s^2x_4^2 - (y_4^2 + x_4^2)(s^2 - x_4^2)}}{x_4^2 + y_4^2} \tag{11}$$

$$x^* = \frac{s^2 - y^2y_4}{x_4} \tag{12}$$

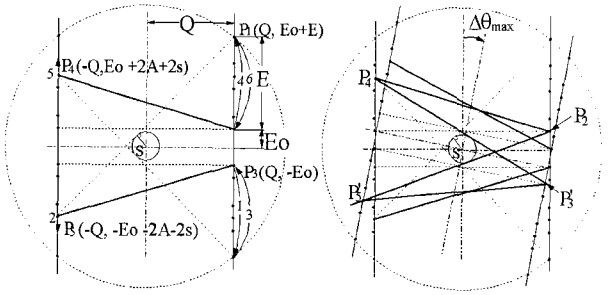

a) b)

Fig. 4. Minimum rotation steps from support pattern# 6 in clockwise rotation(for $E+E_o=5$)
a) rotational gait steps b) Rotated support pattern

Now, consider the support pattern ***1***. Fig. 5a) and 5b) shows the order of movement and actual foothold positions of the four legs of the robot for a rotation of $\Delta\theta$, respectively. At start, the robot is assumed to be at support pattern ***1*** but ends up with support pattern ***4*** and $E_O \neq 0$ after rotational motion. It is also assumed that the robot maintains the given stability margin during rotational motion. It can be seen from Fig. 5(a) and 5(b) that the maximum stability margin equals to the maximum radius of the circle which has its origin at the mass center of the robot and osculates with the line $\overline{Q_1Q_8}$. The maximum radius of the circle can be obtained as

$$d = \frac{Q_s}{\sqrt{(E_o + 3A + 3s)^2 + Q^2}}, \tag{13}$$

where the equation of the line $\overline{Q_1Q_8}$ is

$$y = \frac{E_o + 3A + 3s_{max}}{Q} x + s, \tag{14}$$

It can be noted that from (13), the stability margin of the support pattern ***1*** is smaller than that of the support pattern ***6.*** On the other hand, note that the equation representing the osculating line with the circle of radius of ***d*** with its origin at the mass center of the robot and passing through the point $Q_6(x_6, y_6)$ can be expressed as

$$y = ax + b \tag{15}$$

where

$$a = -\frac{x^*}{y^*} \tag{16}$$

$$b = \frac{x^*}{y^*} x_6 + y_6, \tag{17}$$

$$y^* = \frac{d^2 y_6 \pm d\sqrt{d^2 y_6^2 - (y_6^2 + x_6^2)(d^2 - x_6^2)}}{x_6^2 + y_6^2}, \tag{18}$$

$$x^* = \frac{d^2 - y^* y_6}{x_6} \tag{19}$$

As shown in Fig. 5b), the point Q_2 rotates along the circular path trajectory with its radius of r about the mass center and it can rotate to the point $Q_2'(x_2', y_2')$. The rotated angular displacement represents the maximum angular displacement. The position of the point Q_2 can be obtained as follows:

$$x_2' = \frac{-ab + \sqrt{(ab)^2 - (1+a^2)(b^2 - r^2)}}{(1+a^2)} \tag{20}$$

$$y_2' = a x_2' + b, \tag{21}$$

where

$$r = \sqrt{Q^2 + (E_o + A + 2s)^2} \tag{22}$$

And the obtained maximum angular displacement $\Delta\theta_{max}$ is

$$\Delta\theta_{max} = atan(\frac{y_2'}{x_2'}) - atan(\frac{E_o + A + 2s}{Q}) \tag{23}$$

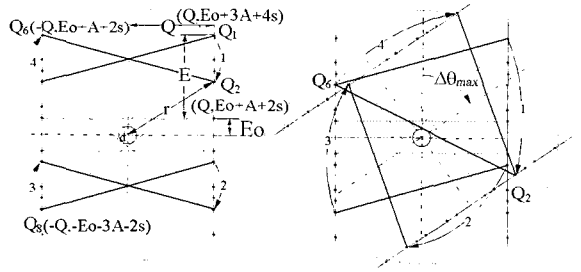

a) b)

Fig. 5. Minimum rotation steps from support pattern # 1 in clockwise rotation(for $E + E_o = 5$).
a) rotational gait steps, b) Rotated support pattern.

Fig. 6a) and 6b), respectively, represents the maximum stability margin and maximum angular displacement when E_o is varied for fixed values of $Q = 5$ and $E + E_O = 5$ from the support pattern *6* and *1*, respectively. It can be confirmed from Fig. 6a) that when the value of $E + E_o$ is fixed, so is the stability margin. But as the value of E_o increases, the maximum angular displacement is decreased. However, for the case of Fig. 6b), both the maximum stability margin and maximum angular displacement are related to the value of E_o. Therefore, contour plot are drawn to represent this relationship. From these plots, it can be confirmed that for the case of the support pattern *6*, as the value of E_o increases, the value of both s_{max} and $\Delta\theta_{max}$ decrease. Also it can be confirmed that for the case of the support pattern *1*, as the value of E_o increases, the value of s_{max} decreases but the value of $\Delta\theta_{max}$ increases.

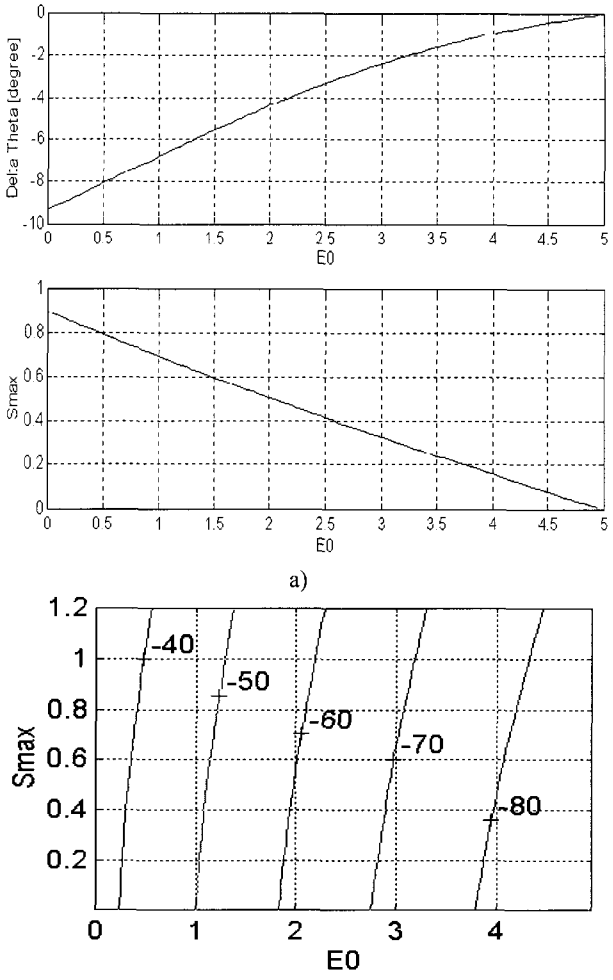

Fig. 6. $\Delta\theta$ Plots for $Q = 5$, $E + E_o = 5$.
a) s_{max}, $\Delta\theta$ plot of Support Pattern 6,
b) $\Delta\theta_{max}$ contour plot of Support Pattern 1 wrt. s_{max} and E_o.

IV. Foothold length E and E_o

In this section, when the location of the first joint axis of each of four legs is placed at a distance e from the mass center of the robot and the value of Q is varied, the magnitudes of foothold lengths E and E_o are investigated.
Fig. 2 represents the projection of the foothold region of each of four legs of the quadruped walking robot to the ground. In the figure, the foothold region of each of four legs is represented as the circle *1, 2, 3,* and *4* as shown in Fig 2.

Fig. 2 represents the robot rotating θ about the z axis.

Denote two lines parallel with the local y axis of the body frame and dislocated an amount of Q from the same axis as $\overline{l_1}$ and $\overline{l_2}$, respectively. The equation of the two lines can be expressed as, respectively,

$$\overline{l_1} : y = mx + c_1 \tag{24}$$

$$\overline{l_2} : y = mx + c_2 \tag{25}$$

where

$$m = -\tan(90^\circ - \theta), \tag{26}$$

$$c_1 = Q\sin\theta + Q\cos\theta\tan(90^\circ - \theta) \tag{27}$$

$$c_2 = -c_1. \tag{28}$$

Also, denote the intersection point between the local x axis and line $\overline{l_1}$ and line $\overline{l_2}$ as P and P', respectively. Then the coordinate of those two points can be expressed as $(Q\cos\theta\ ,\ Q\sin\theta)$ and $(-Q\cos\theta, -Q\sin\theta)$, respectively.

On the other hand, the intersection point (x^*, y^*) between the line $(y = mx + c)$ and the circle of radius R and with its origin at $(a\ ,\ b)$, can be found as

$$x^* = \frac{(mc - mb - a)}{1+m^2} \pm \frac{\sqrt{(mc - mb - a)^2\{a^2 + (b-c)^2 - r^2\}}}{1+m^2} \tag{29}$$

$$y^* = mx^* + c. \tag{30}$$

The intersection between the circles $1,2,3,4$ and the lines $\overline{l_1}$ and $\overline{l_2}$ can be found by inserting the corresponding values to the center of the circle (a,b) and the slope and the intersection of the line (m,c) to (29) and (30). That is, the value for (a,b) to the circles $1,2,3,4$ is $(0,e)$, $(-e,0)$, $(0,-e)$, $(e,0)$, and the slope and the intersection of lines l_1 and l_2 is (m, c_1) and (m, c_2), respectively.

Noting that the quadruped walking robot is symmetric with respect to the mass center of the robot, the complete characteristics on the magnitude of the stride length of the robot at an arbitrary orientation can be represented by examining the range of θ within $0^\circ \le \theta \le 90^\circ$. Fig. 7 and Fig. 8 show two different values of foothold length $\boldsymbol{E}$'s that the walking robot could have after the certain amount of rotational motion of the walking robot ($\Delta\theta < 45^\circ$ and $45^\circ < \Delta\theta < 90^\circ$) is conducted via. regular rotational gaits. Note that in this support patterns the legs are ready to move forward with an angle of $\Delta\theta^\circ$ with respect to the body orientation of the walking robot. First, the range of $\Delta\theta < 45^\circ$ is considered. As it can be seen from Fig. 7a) and 7b), there exist two cases: the point P is within the foothold region of the leg 1, and the point P is out of reachable foothold region of leg 1. Two intersection points between the line l_1 and circle 1 is denoted as M_1 and M_2, respectively, the coordinates of these two points can be found as

$$M_x = \frac{-(mc_1 - me)}{1+m^2} \pm \frac{\sqrt{(mc_1 - me)^2 - (1+m^2)\{(e-c_1)^2 - R^2\}}}{1+m^2} \tag{31}$$

$$M_y = mM_x + c_1. \tag{32}$$

In eqn. (31), the sign of the second term distinguishes the x coordinates of M_1 and M_2. Denote one of intersections between line l_2 and circle 1 as $N(N_x, N_y)$, as in Fig. 7a).

Then the coordinates of the point is written as

$$N_x = \frac{-(mc_2 + e)}{1+m^2} \pm \frac{\sqrt{(mc_2 + e)^2 - (1+m^2)(e^2 + c_2{}^2 - R^2)}}{1+m^2} \tag{33}$$

$$N_y = mN_x + c_2 \tag{34}$$

Therefore, noting that the distance d between the center of the circle $1(0,e)$ and the point $P(P_x, P_y)$ can be written as $d = \sqrt{P_x^2 + (e - P_y)^2}$, the foothold length E and E_o in Fig. 7a) can be expressed as

$$E = \sqrt{(M_{1x} - N_x)^2 + (M_{1y} - N_y)^2 - (2Q)^2} \tag{35}$$

$$E_o = \sqrt{(P_x - M_{1x})^2 + (P_y - M_{1y})^2} \tag{36}$$

Likewise, E and E_o in Fig. 7b) can be written as

$$E_o = \sqrt{(P_x - M_{1x})^2 + (P_y - M_{1y})^2} \tag{37}$$

$$E_o = 0. \tag{38}$$

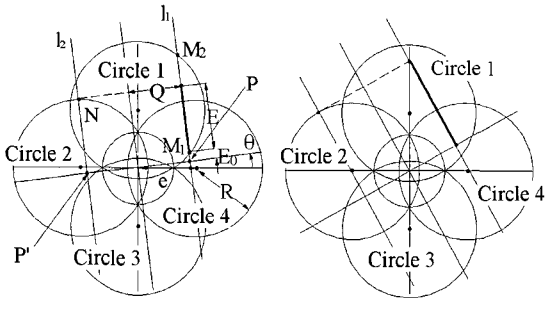

a) b)

Fig. 7. E and E_o Plot for $\Delta\theta > 45^\circ$.
a) $P \not\subset Circle\ 1$, b) $P \subset Circle\ 1$.

On the other hand, when the range of rotational angle is within $\Delta\theta \rangle 45^\circ$, two cases shown in Fig. 8a) and 8b) should be considered. By following the similar procedure, the value of E and E_o corresponding to these cases can be found: that is, for the case of Fig. 8a),

$$E = \sqrt{(P_x - M_{2x})^2 + (P_y - M_{2y})^2}\,, \tag{39}$$

$$E_o = 0\,, \tag{40}$$

and for the case of Fig. 8b),

$$E = \sqrt{(L_x - S_x)^2 + (L_y - S_y)^2 - (2Q)^2} \tag{41}$$

$$E_o = \sqrt{(P_x - L_x)^2 + (P_y - L_y)^2}\,, \tag{42}$$

where

$$L_x = \frac{-(mc_1 - e)}{1+m^2} + \frac{\sqrt{(mc_1 - e)^2 - (1+m^2)(e^2 + c_1^2 - R^2)}}{1+m^2} \tag{43}$$

$$L_x = mL_x + c_1 \tag{44}$$

$$S_x = \frac{-(mc_2 + me)}{1+m^2} + \frac{\sqrt{m^2(e+c_2)^2 - (1+m^2)\{(e+c_2)^2 - R^2\}}}{1+m^2} \tag{45}$$

$$S_y = mS_x + c_2 \tag{46}$$

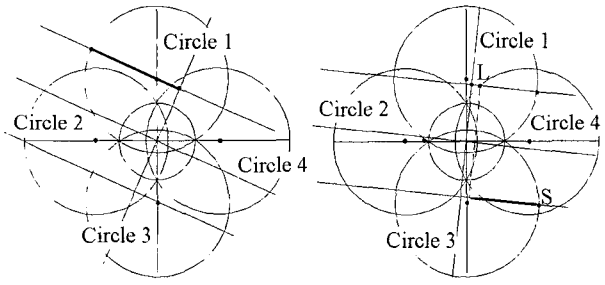

a) b)

Fig. 8. E and E_o Plot for $\Delta\theta > 45^\circ$.
a) $P \subset Circle\ 4$, b) $P \not\subset Circle\ 4$.

From the above analysis it can be seen that the rotation of the quadruped robot is influenced by factors such as E, E_o, and $E + E_o$. Fig. 9a)-c) represent the magnitudes of these factors for the arbitrary orientation of the robot. It can be seen from Fig. 9c) that the value of $E + E_o$ reduces linearly around when $\theta = 45^\circ$.

Fig. 10 represents the maximum stability margin and the magnitude of foothold lengths E and E_0, when $Q = 5$, $R = 7$, and $\theta = 0^\circ$ for the variation of the magnitude of e. It can be seen that from this plot, when $e \approx 4.9$, the robot has the maximum stability margin and maximum foothold length. Fig. 11 a) - 11 d) show the magnitude of the maximum stability margin and the magnitude of foothold length E and E_0 for the case of $Q = 5$, $R = 7$, and

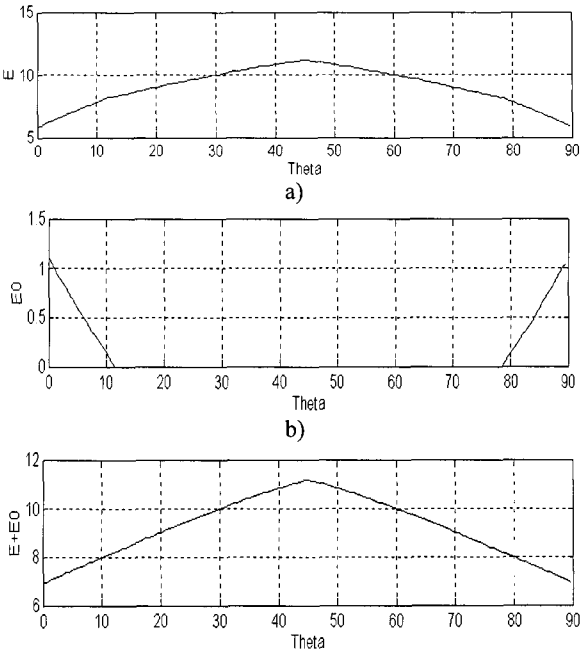

Fig. 9. E vs. θ Plot.
a) E, b) E_o, c) $E + E_o$.

varied values of e (i.e. $e = 0,2,4,6$). From these plots, as the magnitude of e increases, so does the magnitude of E. However, the maximum stability margin does not show significant changes in its magnitude. Also, as can be seen from Fig. 10, around the region of $e < 4.9$ the value of E_0 is always 0, but from Fig. 10 and Fig. 11d), around the region of $e > 4.9$, the value of E_0 has its maximum particularly around region of θ being 0° and 90° and as the magnitude of e increases, the region of $E_0 \neq 0$ is expanded accordingly. As shown in Fig. 11d), since the value of E_0 is not always 0, the maximum stability margin and maximum rotational angle should be carefully investigated.

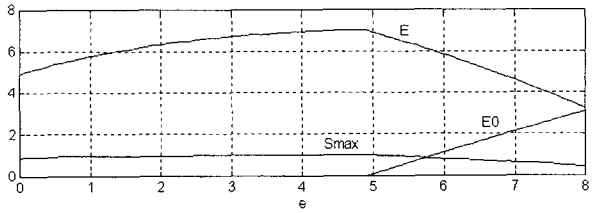

Fig. 10. E and E_0, s_{max} Plot w.r.t. the variation e for $Q = 5$, $R = 7$, and $\theta = 0^\circ$.

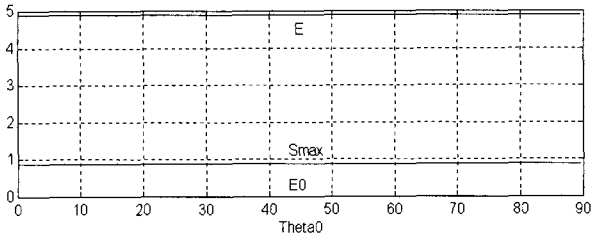

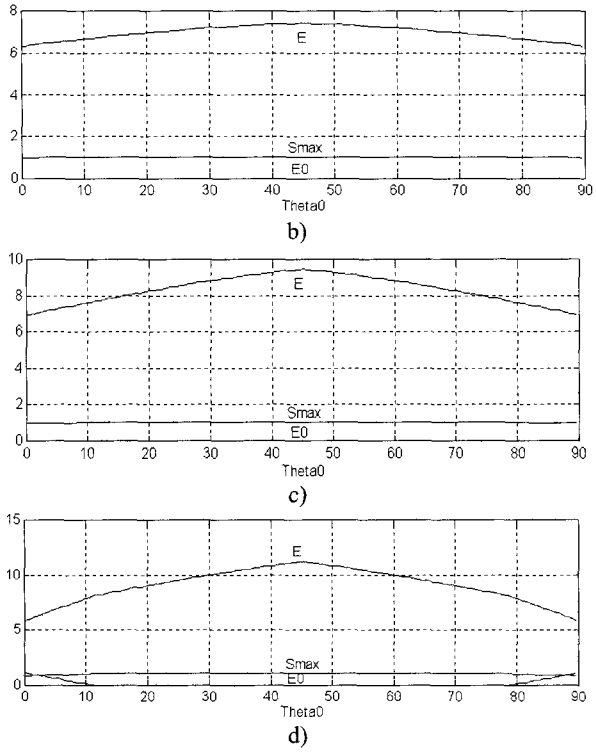

Fig. 11. E, E_0, s_{max} Plot w.r.t. θ.
a) $e=0$, b) $e=2$, c) $e=4$, d) $e=6$.

V. Omni-directional gaits of the quadruped walking robot

First, consider the case when the robot is in support pattern 6 as shown in Fig. 12. In this case, the robot rotates either to clockwise direction or to counter clockwise direction. Note that rotational motions and its characteristics to those two directions are symmetric each other. Therefore, only one direction needs to be considered.

The equations of lines P_4P_3' and $\overline{P_2P_5'}$ can be written as, respectively,

$$y = a_1 x + b_1 \tag{47}$$

$$y = a_2 x + b_2, \tag{48}$$

where

$$a_1 = (y_3' - y_4)/(x_3' - x_4) \tag{49}$$

$$b_1 = y_4 - a_1 x_4 \tag{50}$$

$$a_2 = (y_5' - y_2)/(x_5' - x_2) \tag{51}$$

$$b_2 = y_2 - a_2 x_2 \tag{52}$$

The equations which is necessary to find the osculating point between either of two lines and the circles with its radius of $S_{\max}$ and with its origin at the mass center of the robot can be found as, respectively,

$$x^2 + (a_1 x + b_1)^2 - s_{max}^2 = 0 \tag{53}$$

$$(1 + a_1^2)x^2 + 2a_1 b_1 x + b_1^2 - s_{max}^2 = 0 \tag{54}$$

Noting that either the cases which does not exist osculating points or the cases which exist only one osculating point implies that the robot is capable of rotating from the current orientation by certain amount of rotation angle, say, $\Delta\theta$, this condition can be expressed by the following two equations:

$$D_1 = (a_1 b_1)^2 - (1 + a_1^2)(b_1^2 - s_{max}^2) \le 0, \tag{55}$$

$$D_2 = (a_2 b_2)^2 - (1 + a_2^2)(b_2 - s_{max}^2) \le 0, \tag{56}$$

From Fig. 10b), it can be noted that the coordinates of the point $P_3'(x_3', y_3')$ and the point $P_5'(x_5', y_5')$ can be written as, respectively,

$$x_3' = r_1 \cos(\theta_3 - \Delta\theta), \tag{57}$$

$$y_3' = -r_1 \sin(\theta_3 - \Delta\theta), \tag{58}$$

$$x_5' = -r_2 \cos(\theta_5 + \Delta\theta), \tag{59}$$

$$y_5' = -r_2 \sin(\theta_5 + \Delta\theta), \tag{60}$$

where

$$r_1 = \sqrt{Q^2 + E_o'^2}, \tag{61}$$

$$\theta_3 = a\tan\left(\frac{E_o'}{Q}\right), \tag{62}$$

$$r_2 = \sqrt{Q^2 + (E_o' + 2A' + 2s_{max})^2}, \tag{63}$$

$$\theta_5 = a\tan\left(\frac{E_o' + 2A' + 2s_{max}}{Q}\right), \tag{64}$$

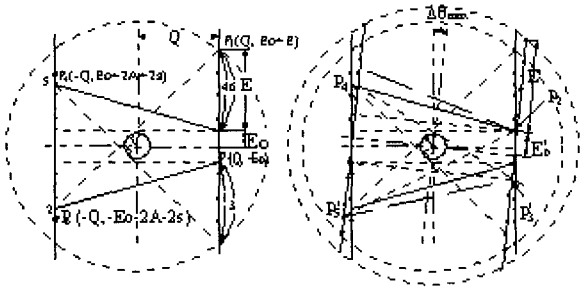

a) b)

Fig. 12. Minimum rotation steps from support pattern # 6 in clockwise rotation.
a) Rotational gait steps, b) Rotated support pattern.

Now, consider the case that the quadruped robot is in support pattern 1. the slope a and the intersection point b of the line which pass through the point Q_6 and $Q_2'(Q_{2x}', Q_{2y}')$ shown in Fig. 13b) can be expressed as

$$a = \frac{Q_{2y}' - Q_{6y}}{Q_{2x}' - aQ_{6x}}, \tag{65}$$

$$b = Q_{6y} - aQ_{6x}, \tag{66}$$

where

$$Q'_{2x} = r\cos(a\tan(\frac{E'_o + A' + 2s}{Q}) + \Delta\theta), \quad (67)$$

$$Q'_{2y} = r\sin(a\tan(\frac{E'_o + A' + 2s}{Q}) + \Delta\theta), \quad (68)$$

$$r = \sqrt{Q^2 + (E'_0 + A' + 2s)}, \quad (69)$$

where and E'_0 and A' represents the foothold length and stride length of the robot, respectively, when it is in orientation angle of $\Delta\theta$. And the condition that the circle of radius of stability margin(d) obtained from (14) and the line $Q_6Q'_2$ do not intersect or has one osculating line can be expressed as

$$D = (ab)^2 - (1+a^2)(b^2 - d^2) \le 0 \quad (70)$$

When this condition is satisfied the robot is capable of rotating $\Delta\theta$.

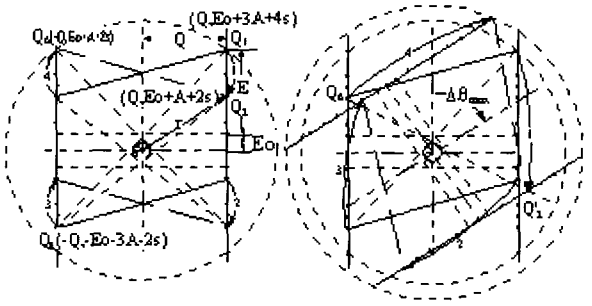

a) b)

Fig. 13. Minimum rotation steps from support pattern # 1 in clockwise rotation.
a) shifting gait steps, b) Rotated support rattern.

Fig. 14a) represents what amount of angles the robot is capable of rotating in clockwise direction when the robot is in arbitrary orientation but in support pattern 6, while maintaining the stability margin obtained in (4). The reason that the rapid change in magnitude of maximum rotational displacement around 11° in the Fig. 14a) is found that in that region the change in value of E_0 allows maximum rotation while not effecting the stability margin too much. Again, as addressed in the above, it can be confirmed that the quadruped walking robot represents symmetric characteristics on every 90° interval due to its symmetric configuration. Fig. 14b) shows the maximum rotational displacement of the robot when it rotates in clockwise direction from the support patter 1 and from the arbitrary orientation, but without affecting the stability margin d obtained in eqn. (14). For the case of support pattern 1, the value of s can be varied from 0 to $E/4$. Particularly, the case of $Q=5$, $R=7$ and $e=6$, that is, which shows the minimum value s_{max} in Fig. 11d), is considered. It can be confirmed that comparing with the support pattern 6, the magnitude of stability margin is reduced $(d < s_{max})$ the magnitude of rotational displacement is increased relatively, on the contrary. In case that the quadruped walking robot, which is in support pattern 1, rotates in counter clockwise direction, the similar method can be applied therefore, in this paper its detailed procedure is not discussed.

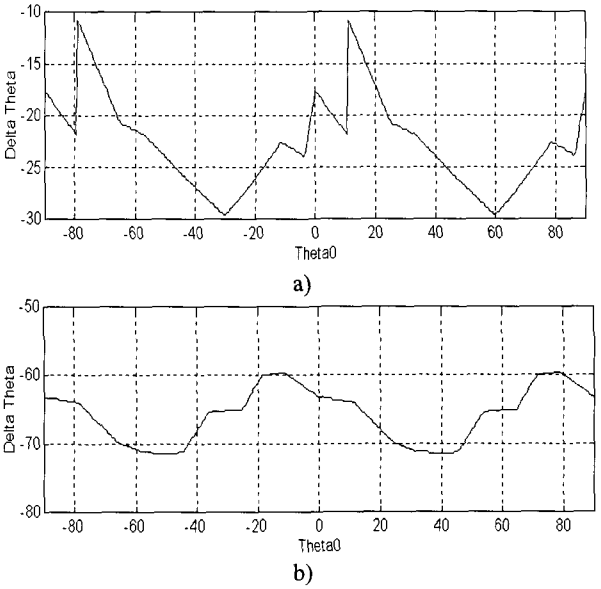

Fig. 14. $\Delta\theta_{max}$ vs. $\Delta\theta$ Plot in clockwise rotation of
a) Support pattern # 6, b) Support pattern # 1.

VI. Conclusion

In this paper, the regular rotational gaits of the quadruped walking robot is investigated. Each of four legs of the quadruped walking robot consists of three RPP type joints and its body fixed revolute joint is located the distance e from the mass center of the robot. The contributions and results from this study can be summarized as below:

1) The regular rotational gaits for the quadruped walking robot is proposed. The rotational gait starts in one of six support patterns of the regular translational gaits[1] and ends in one of six support patterns of the regular translational gait. Thus, transitional step between rotational gait and translational gait do not exist. Also, note that the orientation of the robot is not changed even after performing the proposed regular rotational gaits: only foothold positions of the robot may be changed.

2) Two representative support patterns out of six support patterns in regular translational gaits of the robot are considered. The effects of Q, E and E_0 to the maximum stability margin s_{max} and maximum rotational displacement $\Delta\theta_{max}$ for these two support patterns are throughly investigated. Particularly, when the larger angular change of the robot than the allowed maximum rotational displacement of the robot is required, it can be accomplished by sequentially performing regular rotational gaits until the desired rotation is completed.

It can be noted from this study that the quadruped walking robot has non-isotropic characteristics. Thus, the walking robot needs to be oriented properly through the proposed rotational gait so that the robot has the largest stride length to move at highest speed as possible. Currently, the dynamic

stability of the robot in addition to the static stability is now under study.

References

[1] T. T. Lee, and C. L. Shih, "A Study of the gait control of a quadruped walking vehicle," *IEEE Journal of Robotics and Automation*, vol. RA-2, no. 2, pp. 61-69, 1986.

[2] B. S. Lin, and S. M. Song, "Dynamic modeling, stability and energy efficiency of a quadrupedal walking machine," *Proc. of IEEE R & A Conf.*, pp. 367-373, 1993.

[3] J. Furusho, and A. Sano, "Sensor-based control of a nine-link biped," *The International Journal of Robotics Research*, vol. 9, no. 2, pp. 83-98, 1990.

[4] J. Furusho, A. Sano, M. Sakaguchi, and E. Koizumi, "Realization of bounce gait in a quadruped robot with articular-joint-type legs, "*Proc. of IEEE R&A conf.*, pp. 697-702, 1995.

[5] J. Hodgins, J. Koechling, and M.H. Raibert, "Running experiments with a planar biped," *Robotics Research 3, ch. 8. MIT press*, pp. 349-355, 1984.

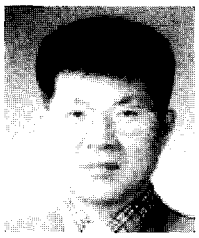

Wheekuk Kim

Mechanical Engineering, at Korea University, Seoul, Korea, in 1980 and M.S. and Ph.D. degrees in Department of Mechanical Engineering, at the University of Texas, at Austin, in 1985 and 1990, respectively. Currently, he is a professor of the Department of Control and Instrumentation Engineering, Korea University. His current research interests are in the area of design of parallel robots, kinematic/dynamic modeling and analysis of parallel/mobile/walking robots.

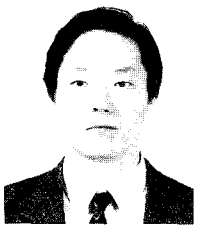

Whang Cho

Mechanical Engineering, at Kwang woon University, Seoul, Korea, in 1981 and M.S. and Ph.D. degrees in Department of Mechanical Engineering, at the University of Texas, at Austin, in 1986 and 1990, respectively. Currently, he is a professor of the Department of Control and Instrumentation Engineering, Kwangwoon University. His current research interests are in the area of modeling and behaviour-based control of general dynamic systems.

Byung-Ju Yi

He received BS degree in Department of Mechanical Engineering from Hanyang University and M.S. and Ph.D. in Department of Mechanical Engineering, at the University of Texas, at Austin, in 1986 and 1991, respectively. Currently, he is an associate professor of School of Electrical Engineering and Computer Science, Hanyang University. His current research interests are in kinematic/dynamic modeling and analysis of general robotic systems with applications to parallel system, mobile system, and haptic interface device.